

# SCIENTIFIC REPORTS

OPEN

## LC-MS guided isolation of three pairs of enantiomeric alkaloids from *Macleaya cordata* and their enantioseparations, antiproliferative activity, apoptosis-inducing property

Chunmei Sai<sup>1,2</sup>, Dahong Li<sup>2</sup>, Shengge Li<sup>2</sup>, Tong Han<sup>2</sup>, Yongzhi Guo<sup>2</sup>, Zhanlin Li<sup>2</sup> & Huiming Hua<sup>2</sup>

(±)-Macleayins F–H (1–3), three pairs of new enantiomeric alkaloid dimers, along with four known alkaloids (4–7) as their plausible biogenetic precursors, were isolated from the aerial parts of *Macleaya cordata*. Compounds 1–3 were obtained under the guidance of LC-MS investigation, and their structures were elucidated by analysis of the 1D and 2D NMR spectroscopic data. The racemic mixtures were successfully separated by chiral HPLC, and the absolute configurations of enantiomers were determined by electronic circular dichroism (ECD) spectroscopy. Compounds 1–7 showed antiproliferative activity against HL-60 with IC<sub>50</sub> values of 1.34–41.30 μM, especially compounds 1–2 exhibited the best inhibitory activity against HL-60 cell lines. In addition, the preliminary mechanism investigation for compound 2 using Annexin V/7-AAD double-staining assay, DAPI staining assay and JC-1 staining method, indicated that 2 inhibited cancer cell proliferation potentially through inducing apoptosis *via* the mitochondria-related pathway and arrested cell cycle of HL-60 cells at S phase.

Benzophenanthridine and protopine alkaloids occur in *Macleaya cordata* (Willd) R. Br. and have been investigated for their intriguing bioactivity, such as anticancer, anti-bacterial, insecticidal, and anti-inflammatory effects<sup>1,2</sup>. *Macleaya cordata* is a perennial plant in the family of Papaveraceae, which has been used in folk medicine for the treatment of cervical cancer, thyroid cancer, inflamed wounds, ringworm infection, arthritis, and trichomonas vaginalis<sup>3,4</sup>. In our previous investigation, two pairs of enantiomeric alkaloid dimers (macleayins A and B) with cytotoxicity were isolated from *M. cordata*<sup>5</sup>. In our present study, LC-MS-guided fractionation (Fig. 1) led to the isolation of three pairs of analogous dimers, macleayins F–H (1–3) biogenetically derived from a benzophenanthridine and protopine alkaloid through C6–C<sub>13</sub> linkage. Four possible biogenetic precursors, sanguinarine, chelerythrine, protopine, and allocryptopine (4–7) were obtained (Fig. 2). Herein, we reported the isolation, and structural elucidation of new compounds. In addition, the antiproliferative properties and action mechanism were also investigated.

### Results and Discussion

**Structural Elucidation of Compounds 1a/1b–3a/3b.** Macleayin F (1) was isolated as white amorphous powder, with the molecular formula of C<sub>41</sub>H<sub>36</sub>N<sub>2</sub>O<sub>9</sub>, deduced from HRESIMS [M + H]<sup>+</sup> (*m/z* 701.2491, calcd for 701.2494), appropriate for 25 degrees of unsaturation. The IR spectrum indicated the presence of ketone carbonyl (1656 cm<sup>-1</sup>), methylenedioxy group (2792, 941 cm<sup>-1</sup>), and aromatic ring (1616, 1486, 1462 cm<sup>-1</sup>). In the UV spectrum, the absorption maxima at 227 and 287 nm were detected. The HRESIMS/MS spectrum exhibited the

<sup>1</sup>School of Pharmacy, Jining Medical University, Rizhao, 276826, Shandong Province, People's Republic of China.

<sup>2</sup>Key Laboratory of Structure-Based Drug Design and Discovery, Ministry of Education, Shenyang Pharmaceutical University, Shenyang, 110016, Liaoning Province, People's Republic of China. Correspondence and requests for materials should be addressed to C.S. (email: saichunmei1980@163.com) or Z.L. (email: lzl1030@hotmail.com) or H.H. (email: huimhua@163.com)

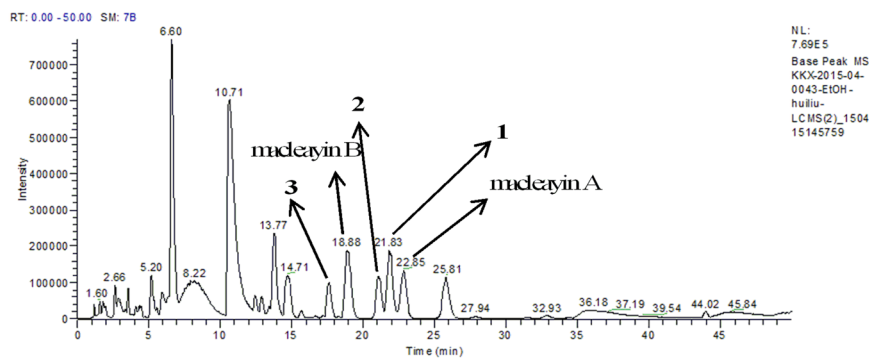


**Figure 1.** LC-MS analysis chromatogram of the crude ethanol extract from *M. cordata*.

fragment peak at  $m/z$  348.1281 assigned to chelerythrine<sup>6</sup>. The  $^1\text{H}$  NMR (Table 1) spectrum revealed the presence of three AB spin systems of aromatic protons in *ortho*-position ( $\delta_{\text{H}}$  6.68 (br d,  $J = 7.3$  Hz, H-9) and 7.23 (br d,  $J = 7.3$  Hz, H-10), 7.46 (d,  $J = 8.5$  Hz, H-12) and 7.61 (d,  $J = 8.5$  Hz, H-11), 6.97 (br d,  $J = 8.0$  Hz, H-11') and 7.50 (br s, H-12')), four aromatic protons in singlet ( $\delta_{\text{H}}$  7.05, 6.85, 6.83, and 6.21), two  $\text{sp}^3$  methine protons ( $\delta_{\text{H}}$  5.13 (d,  $J = 9.0$  Hz) and 4.59 (d,  $J = 9.0$  Hz)), as well as three methylenedioxy groups ( $\delta_{\text{H}}$  5.99 (d,  $J = 1.1$  Hz), 5.96 (d,  $J = 1.1$  Hz), 5.91 (d,  $J = 1.1$  Hz), 5.83 (d,  $J = 1.1$  Hz), 5.87 (d,  $J = 1.4$  Hz), and 5.82 (d,  $J = 1.4$  Hz)), two methoxy groups ( $\delta_{\text{H}}$  3.94 and 3.83), and two *N*-methyl groups ( $\delta_{\text{H}}$  2.51 and 1.63). The  $^{13}\text{C}$  NMR (Table 1) combined with the HSQC spectroscopic data identified twenty-eight aromatic, three methylenedioxy, two methoxy, two *N*-methyl, three methylene, and two  $\text{sp}^3$  methine carbons (Table 1). Considered its molecular formula, one carbonyl carbon signal was absent in its  $^{13}\text{C}$  NMR spectrum. The above data suggested that **1** was a dimeric alkaloid consisting of a chelerythrine and a protopine moiety<sup>5</sup>.

The HMBC correlations (Fig. 3) of H-1/C-3, C-4a, C-12; H-10/C-6a, C-8; H-11/C-4b, C-10a, C-12a; H-12/C-1, C-4a, C-10b; 7-OCH<sub>3</sub>/C-7; 8-OCH<sub>3</sub>/C-8; -NCH<sub>3</sub>/C-4b, and from the protons of OCH<sub>2</sub>O ( $\delta_{\text{H}}$  5.99 and 5.96) to C-2, and C-3, as well as the  $^1\text{H}$ - $^1\text{H}$  COSY correlations (Fig. 3) of H-9/H-10 and H-11/H-12, evidenced the presence of chelerythrine moiety. This was furthermore confirmed by the fragment peak at  $m/z$  348.1281 in the HRESIMS/MS (Supplementary Figure S13). In the  $^1\text{H}$  NMR spectra of **1**, the signals in the high field region were substantially overlapped. Hence, the presence of protopine structure could not be completely assigned with the observed HMBC cross-peaks of H-1'/C-3', C-4'a; H-4'/C-2', C-5', C-14'a; H-11'/C-9', C-10', C-12'a; as well as cross-peaks of two methylenedioxy at  $\delta_{\text{H}}$  5.91, 5.83/C-2', C-3' and  $\delta_{\text{H}}$  5.87, 5.82/C-9', C-10'. Comparison of the NMR and HRESIMS data of **1** with those of macleayins A and B<sup>5</sup> which were previously obtained as a single crystal molecule from *M. cordata* indicated that **1** and macleayin B possessed protopine moiety. In addition, the  $^1\text{H}$ - $^1\text{H}$  COSY of H-6/H-13' proved the direct linkage of C6-C13'. Similarly, one carbonyl and several crucial HMBC correlations were not observed in **1**. Accordingly, the planar structure of compound **1** was defined as shown.

The relative stereochemistry of **1** was established by the NOESY experiment (Fig. 3). The coupling constant ( $J = 9.0$  Hz) and no NOE correlation between H-6 and H-13', suggested that H-6 and H-13' may be on the opposite side. The proposed relative stereochemistry is a reasonable hypothesis, as well as the fact that this is due to the lacunar nature of the available data set. Compound **1** was a racemic mixture like macleayins A and B due to the lack of optical rotation and Cotton effect (CE)<sup>7</sup>. Subsequently, the enantioseparation of **1** was performed on a chiral column (Daicel Chiralpak IB) to yield the enantiomers **1a** and **1b** in an approximate 1:1 ratio (Supplementary Figure S4)<sup>8</sup>, which were opposite in terms of optical rotation (**1a**:  $[\alpha]_{\text{D}}^{20} + 274$  ( $c$  0.07, MeOH), **1b**:  $[\alpha]_{\text{D}}^{20} - 248$  ( $c$  0.07, MeOH)). The assignments of their absolute configuration at the stereogenic centers were determined by comparing the ECD spectra (Fig. 4) of both enantiomers with those of two similar compounds (+)-macleayin A and (-)-macleayin A. The measured ECD curves of **1a** and **1b** matched with that of (6*R*,13'*R*)-macleayin A and (6*S*,13'*S*)-macleayin A, respectively. Hence, the absolute configuration for **1a** (6*R*,13'*R*) and **1b** (6*S*,13'*S*) were unambiguously determined as shown in Fig. 1 and named (+)-macleayin F and (-)-macleayin F, respectively.

Macleayin G (**2**) was obtained as white amorphous powder. The molecular formula of **2** was established as C<sub>42</sub>H<sub>40</sub>N<sub>2</sub>O<sub>9</sub> on the basis of positive HRESIMS at  $m/z$  717.2799 [ $\text{M} + \text{H}$ ]<sup>+</sup> (calcd 717.2807), indicating 24 indices of hydrogen deficiency. The IR spectrum showed absorption bands due to ketone carbonyl (1652 cm<sup>-1</sup>), methylenedioxy group (2794, 938 cm<sup>-1</sup>), and aromatic ring (1619, 1491, 1458 cm<sup>-1</sup>) functionalities. The UV spectrum exhibited maximum absorption at 229 and 286 nm. Its  $^1\text{H}$  and  $^{13}\text{C}$  NMR data (Table 1) revealed structural similarity to **1**, expected that one methylenedioxy in **1** was replaced by two methoxy groups ( $\delta_{\text{H}}$  3.95, 3.50;  $\delta_{\text{C}}$  56.0, 60.9). It was confirmed by the HMBC correlations of 8-OCH<sub>3</sub> with C-8, 7-OCH<sub>3</sub>/H-6 with C-7; 9'-OCH<sub>3</sub>/H-8'/H-11' with C-9', and of 10'-OCH<sub>3</sub>/H-11' with C-10' (Supplementary Figure S2). Furthermore, the HRESIMS/MS showed the fragment ion peak at  $m/z$  348.1306 which was recognized as chelerythrine, suggested that **2** was made up of chelerythrine and allocryptopine, which was supported by comparison of NMR data of **2** with those of macleayin B<sup>5</sup>.  $^1\text{H}$ - $^1\text{H}$  COSY correlations (Supplementary Figure S2) of H-6/H-13' confirmed that two parts were connected by C-6 with C-13'. Similarly, compound **2** was proposed to be a racemic mixture on account of the lack of optical rotation and CE. Subsequently, **2a** and **2b** were obtained by chiral-phase HPLC separation in a ratio of 1:1 (Supplementary Figure S5), which exhibited the mirror image-like ECD curves and owned the opposite

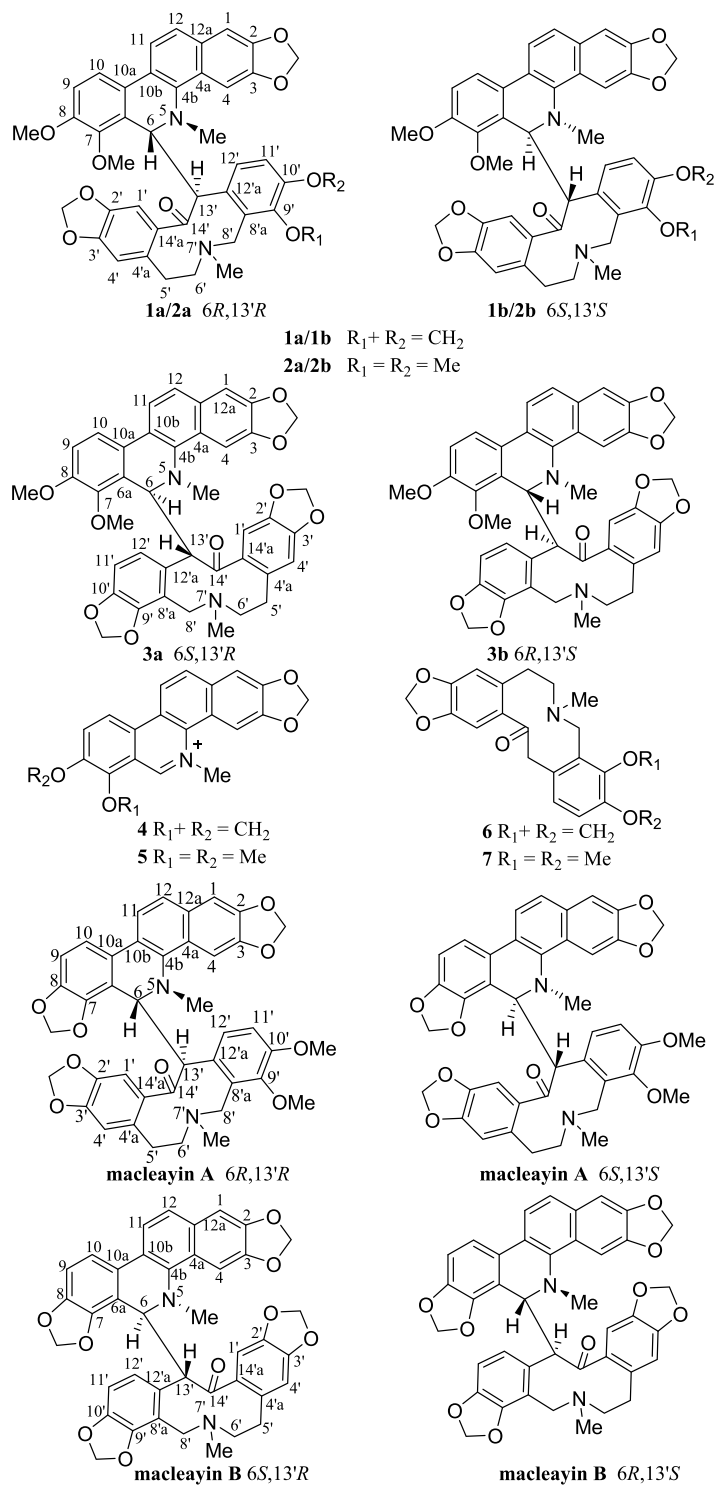


**Figure 2.** Structures of compounds **1–7** and macleayins **A, B**.

specific optical rotations (**2a**:  $[\alpha]_{\text{D}}^{20} + 238$  (*c* 0.10 MeOH)), **2b**:  $[\alpha]_{\text{D}}^{20} - 210$  (*c* 0.10 MeOH)). Thus, the absolute configuration of **2a** and **2b** were assigned as (6*R*,13'*R*) and (6*S*,13'*S*) by comparing their experimental ECD spectra with those of (+)-macleayin A and (–)-macleayin A (Fig. 4), and given the names (+)-macleayin G and (–)-macleayin G, respectively.

Macleayin H (**3**) was isolated as white amorphous powder and yielded a quasi-molecular ion peak at  $m/z$  701.2485  $[\text{M} + \text{H}]^+$  (calcd for 701.2494) in the HRESIMS, indicative of molecular formula  $\text{C}_{41}\text{H}_{36}\text{N}_2\text{O}_9$ , the same as that of **1**. The identical fragment peak at  $m/z$  348.1323 in HRESIMS/MS as **1**, together with 1D and 2D NMR data (Table 1) deduced that **3** was a similar dimer comprising chelerythrine and protopine as **1**. But the chemical shifts of H-4 and H-4' in compound **3** were significantly shifted upfield (ca.  $-1.6$  and  $-0.3$  ppm), and H-13' was

| No.   | 1  |                     | 2  |                     | 3  |                     |
|---|--|---------------------|--|---------------------|--|---------------------|
|   | $\delta_{\text{H}}$ (mult., $J$ , in Hz) | $\delta_{\text{C}}$ | $\delta_{\text{H}}$ (mult., $J$ , in Hz) | $\delta_{\text{C}}$ | $\delta_{\text{H}}$ (multi, $J$ , in Hz) | $\delta_{\text{C}}$ |
| 1   | 7.05 (s)                                 | 104.2               | 7.03 (s)                                 | 104.1               | 7.01 (s)                                 | 104.0               |
| 2   |  | 147.5               |  | 147.4               |  | 147.2               |
| 3   |  | 147.9               |  | 148.0               |  | 147.4               |
| 4   | 6.85 (s)                                 | 100.8               | 6.77 (s)                                 | 100.8               | 5.29 (br s)                              | 100.5               |
| 4a  |  | 127.6               |  | 127.8               |  | 127.1               |
| 4b  |  | 139.4               |  | 139.4               |  | 139.5               |
| 6   | 5.13 (d, 9.0)                            | 58.0                | 5.14 (d, 10.3)                           | 57.8                | — <sup>a</sup>                           | 63.8                |
| 6a  |  | 126.7               |  | 127.0               |  | 125.6               |
| 7   |  | 146.3               |  | 146.3               |  | 146.8               |
| 8   |  | 152.1               |  | 152.0               |  | 152.1               |
| 9   | 6.68 (br d, 7.3)                         | 111.7               | 6.66 (br s)                              | 111.5               | 6.84 (d, 8.4)                            | 112.6               |
| 10  | 7.23 (br d, 7.3)                         | 116.6               | 7.23 (br s)                              | 118.5               | 7.39 (d, 8.4)                            | 118.9               |
| 10a   |  | 125.0               |  | 125.0               |  | 125.4               |
| 10b   |  | 124.3               |  | 124.5               |  | 124.0               |
| 11  | 7.61 (d, 8.5)                            | 119.8               | 7.63 (d, 8.5)                            | 119.9               | 7.78 (d, 8.4)                            | 119.8               |
| 12  | 7.46 (d, 8.5)                            | 123.8               | 7.45 (d, 8.5)                            | 123.7               | 7.48 (d, 8.4)                            | 124.2               |
| 12a   |  | 131.0               |  | 130.8               |  | 130.9               |
| 1'  | 6.83 (s)                                 | 111.7               | 6.92 (s)                                 | 112.1               | — <sup>a</sup>                           | — <sup>a</sup>      |
| 2'  |  | 145.6               |  | 145.4               |  | — <sup>a</sup>      |
| 3'  |  | 148.3               |  | 147.8               |  | — <sup>a</sup>      |
| 4'  | 6.21 (s)                                 | 109.8               | 6.19 (s)                                 | 109.7               | 5.89 (s)                                 | 110.8               |
| 4'a   |  | 133.7               |  | 134.1               |  | — <sup>a</sup>      |
| 5'  | 2.37–2.31 (m) 1.93 (br s)                | 33.4                | 2.50–2.33 (m) 1.86–1.65 (m)              | 33.7                | 2.23–1.59 (m)                            | — <sup>a</sup>      |
| 6'  | 2.37–2.31 (m) 1.85 (br s)                | 56.9                | 2.50–2.33 (m) 1.86–1.65 (m)              | 57.2                | 2.23–1.59 (m)                            | — <sup>a</sup>      |
| 8'  | 3.07 (d, 13.2) 2.32 (br s)               | 48.5                | 3.09 (d, 13.3) 2.50–2.33 (m)             | 48.3                | 3.21 (br s) 3.02 (br s)                  | — <sup>a</sup>      |
| 8'a   |  | 118.5               |  | 130.6               |  | — <sup>a</sup>      |
| 9'  |  | 145.0               |  | 147.0               |  | — <sup>a</sup>      |
| 10'   |  | 146.0               |  | 150.5               |  | 150.1               |
| 11'   | 6.97 (br d, 8.0)                         | 107.1               | 7.07 (d, 8.3)                            | 110.8               | 6.81 (d, 6.6)                            | 107.7               |
| 12'   | 7.50 (br s)                              | 122.5               | 7.61 (d, 8.3)                            | 125.2               | 7.83 (br s)                              | — <sup>a</sup>      |
| 12'a  |  | 132.9               |  | 132.1               |  | — <sup>a</sup>      |
| 13'   | 4.59 (d, 9.0)                            | 52.8                | 4.47(d, 10.3)                            | 52.9                | 5.01 (br s)                              | — <sup>a</sup>      |
| 14'   |  | — <sup>a</sup>      |  | — <sup>a</sup>      |  | — <sup>a</sup>      |
| 14'a  |  | 135.5               |  | 135.6               |  | — <sup>a</sup>      |
| 5-N-CH <sub>3</sub>                             | 2.51 (s)                                 | 41.1                | 2.50 (s)                                 | 40.8                | 2.56 (s)                                 | 43.1                |
| 7'-N-CH <sub>3</sub>                            | 1.63 (s)                                 | 41.7                | 1.49 (s)                                 | 41.5                | 1.89 (s)                                 | 41.4                |
| 2,3-OCH <sub>2</sub> O-                         | 5.99 (d, 1.1) 5.96 (d, 1.1)              | 101.1               | 5.93–5.81 (m)                            | 101.0               | 5.99–5.76 (m)                            | 101.1               |
| 7-OCH <sub>3</sub>                              | 3.94 (s)                                 | 61.0                | 3.93 (s)                                 | 61.8                | 3.77 (s)                                 | 61.1                |
| 8-OCH <sub>3</sub>                              | 3.83 (s)                                 | 55.9                | 3.81 (s)                                 | 55.7                | 3.65 (s)                                 | 56.1                |
| 2',3'-OCH <sub>2</sub> O-                       | 5.91 (d, 1.1) 5.83 (d, 1.1)              | 101.1               | 5.93–5.81 (m)                            | 100.9               | 5.99–5.76 (m)                            | 101.6               |
| 9',10'-OCH <sub>2</sub> O- or -OCH <sub>3</sub> | 5.87 (d, 1.4) 5.82 (d, 1.4)              | 100.6               | 3.50 (s) 3.95 (s)                        | 60.9 56.0           | 5.99–5.76 (m)                            | 100.9               |

**Table 1.** <sup>1</sup>H [600 MHz,  $\delta$  in ppm, Mult. ( $J$  in Hz)] and <sup>13</sup>C NMR (150 MHz,  $\delta$  in ppm) data of 1–3 in CDCl<sub>3</sub>. —<sup>a</sup>No signal observed in <sup>1</sup>H NMR and <sup>13</sup>C NMR spectra.

shifted downfield (ca. +0.4 ppm). Compound **3** showed more similar NMR data (Supplementary Tables S1 and S2) to macleayin B than **1**, deducing that the relative configuration of **3** was the same as macleayin B. Subsequent chiral HPLC resolution (Supplementary Figure S6) of **3** afforded **3a** ( $[\alpha]_{\text{D}}^{20} + 71$  (c 0.11 MeOH)) and **3b** ( $[\alpha]_{\text{D}}^{20} - 94$  (c 0.11 MeOH)). The absolute configuration at the stereocenters of **3a** (6*S*,13'*R*) and **3b** (6*R*,13'*S*) were established by comparison of their experimental ECD spectra with those of (+)-macleayin B and (–)-macleayin A (Fig. 4), and named (+)-macleayin H, and (–)-macleayin H, respectively.

**Antiproliferative activity.** Our previous study revealed that alkaloids from *M. cordata* exhibited promising antiproliferative effects, so all the isolated compounds were tested for the growth inhibitory activities against HL-60, A-549, MCF-7 human cancer cell lines by the trypan blue method and MTT method<sup>9,10</sup>. The results were summarized in Table 2. All compounds inhibited the growth against all the tested cancer cells with IC<sub>50</sub> values ranged from 1.34 to 41.30  $\mu$ M. In particular, **1a**, **1b**, **2a**, and **2b** showed more potent antiproliferative property against HL-60 cell lines than their biogenetic precursors **5–7**, and the enantiomers displayed similar inhibitory

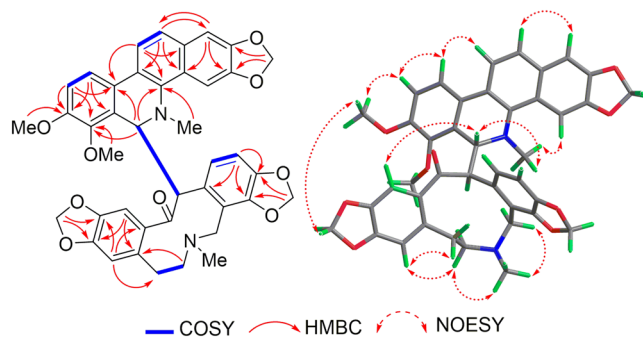


**Figure 3.** HMBC,  $^1\text{H}$ - $^1\text{H}$  COSY, and NOESY correlations of macleayin F (1).

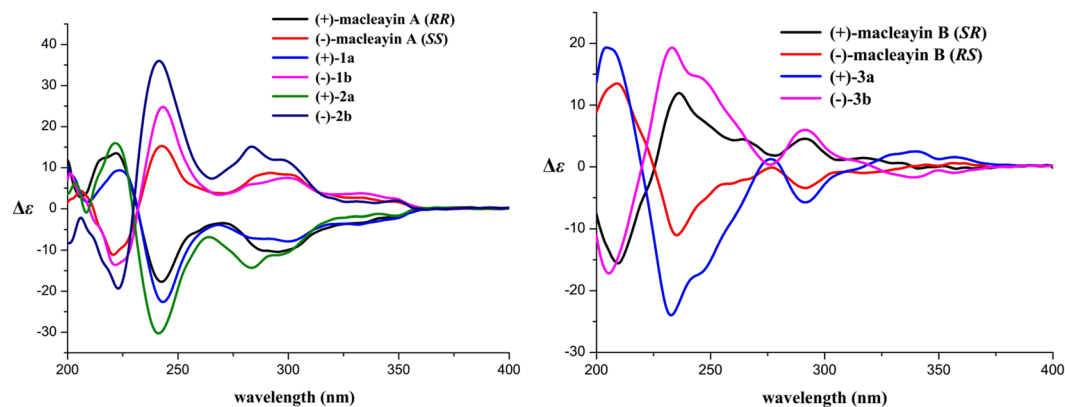


**Figure 4.** CD spectra for compounds 1a, 1b, 2a, 2b, 3a, 3b, and (+)-/(-)-macleayin A, (+)-/(-)-macleayin B.

| Comp. | IC <sub>50</sub> (μM) |              |              |
|-------|-----------------------|--------------|--------------|
|       | HL-60                 | A-549        | MCF-7        |
| 1a    | 1.70 ± 0.89           | 10.98 ± 1.93 | 25.78 ± 0.88 |
| 1b    | 1.34 ± 1.02           |              |              |
| 2a    | 3.35 ± 0.13           | 9.87 ± 1.08  | 12.29 ± 1.06 |
| 2b    | 2.47 ± 0.56           |              |              |
| 3a    | 6.49 ± 1.24           | 41.30 ± 0.29 | 18.88 ± 0.99 |
| 3b    | 8.37 ± 0.26           |              |              |
| 4     | 7.71 ± 0.78           | 8.49 ± 0.63  | 5.51 ± 1.42  |
| 5     | 9.61 ± 2.45           | 9.38 ± 0.91  | 7.74 ± 2.75  |
| 6     | 8.94 ± 0.37           | 27.37 ± 1.05 | 25.19 ± 3.09 |
| 7     | 7.18 ± 1.03           | 26.06 ± 0.58 | 28.24 ± 1.64 |
| 5-Fu  | 2.8 ± 2.03            | 1.6 ± 1.22   | 17.01 ± 0.95 |

**Table 2.** The antiproliferative activity of compounds 1–7. IC<sub>50</sub> is the concentration that inhibited 50% of cell growth. Results are expressed as the mean ± SD of three independent experiments.

effects. Therefore, compound 2 was selected for further investigation on the antiproliferative mechanism in HL-60 cells.

**Influence of compound 2 on the HL-60 cell cycle.** Cell cycle arrest was an important sign for inhibition of proliferation and the series of events that took place in a cell leading to its division and duplication<sup>11,12</sup>. In order to explore whether the growth inhibition induced by 2 was caused by the regulation of the HL-60 cell cycle, the cell cycle distribution in the presence of 2 was detected by flow cytometry (Fig. 5). HL-60 cells were treated with compound 2 at concentrations of 3.75, 7.5, and 15.0 μM for 72 h, which resulted in a remarkable increase of 31.49%, 46.11%, and 48.36% of cells at S phase compared with that of the control (28.00%), while there was a concomitant decline in the number of cells in G1 and G2 phases. This information indicated that compound 2 influenced cell cycle of HL-60 arrested at S phase in a dose-dependent manner.

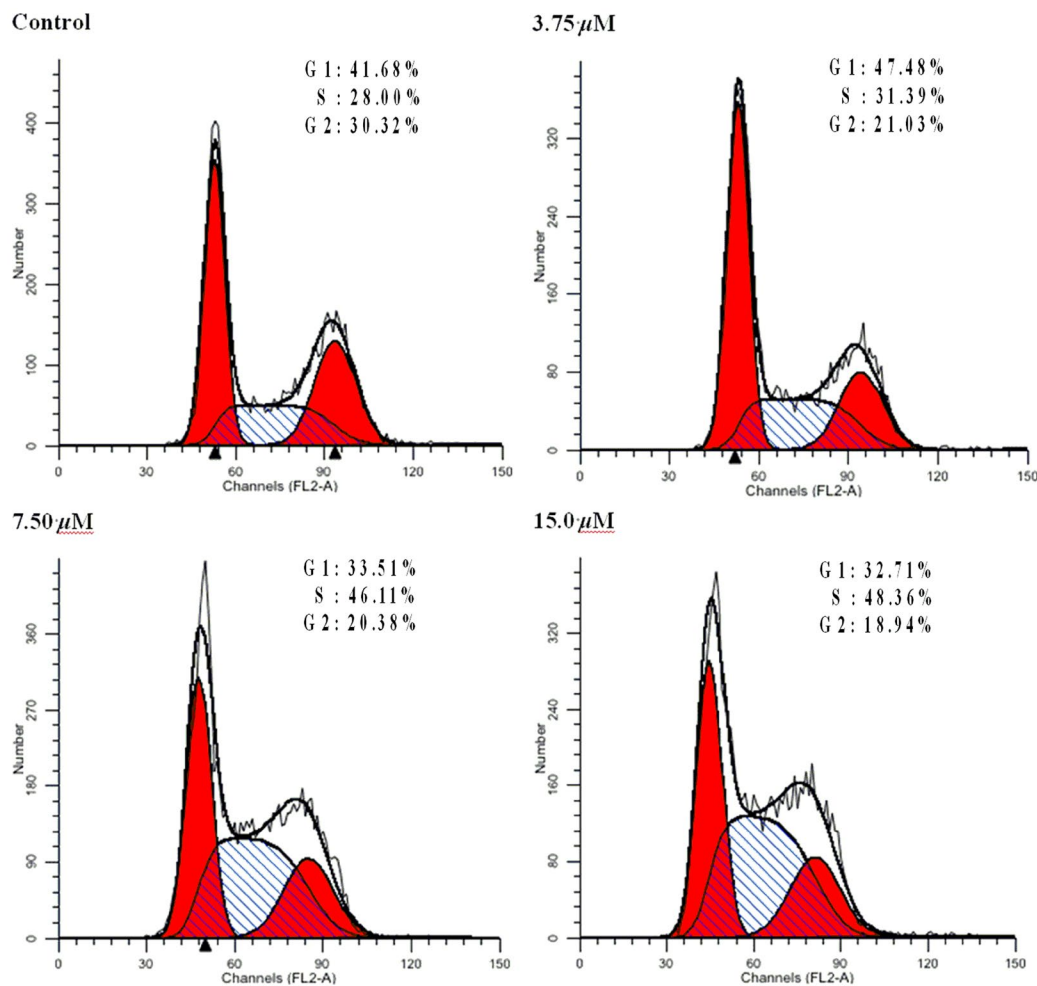


**Figure 5.** The influence of HL-60 cell cycle by compound **2**. Left red part: cell in G1 phase; Right red part: cell in G2 phase; Oblique line part: cell in S phase; White part: total cells.

**Induction of apoptosis by compound **2**.** Apoptosis is an ordered and orchestrated cellular process that takes place in physiological and pathological conditions<sup>13,14</sup>. Therefore, drug-induced apoptosis in tumor cells is important for cancer treatment. The effects of **2** on the apoptosis of HL-60 cells by staining them with Annexin-V APC/7-AAD and analysis by flow cytometry were examined. As shown in Fig. 6, the treatment with 3.75, 7.50, and 15.0 μM of **2** for 72 h in HL-60 cells, the total percentage of early apoptotic cells (right low quadrant) and late apoptotic and necrotic cells (right upper quadrant) were increased from 5.41% to 61.34%. The data indicated that compound **2** remarkably induced apoptotic cells death in HL-60 cells in a concentration-dependent manner.

**Effect of mitochondria depolarization by compound **2**.** The destruction of mitochondrial membrane potential is widely considered to be a crucial event in the process of cell apoptosis<sup>15,16</sup>. In order to further research the apoptosis induced effect of compound **2**, the fluorescent probe JC-1 was carried out to detect the changes of mitochondrial membrane potential. JC-1 (a kind of lipophilic cationic dye) can pass the plasma membrane into cells and accumulate in mitochondria. Meanwhile, membrane potential and degree of accumulation of JC-1 in mitochondria exist close contact. Normal cells, normal membrane potential, at the higher concentration of dye JC-1, with the dye aggregation, fluorescence emission gradually changes red. While apoptotic cells, the mitochondrial transmembrane potential depolarization, the monomer of JC-1 is formed, and fluorescence emission changes from red to green. Therefore, it can easily be used to test the changes of mitochondrial membrane potential by detecting the changes of fluorescence color. HL-60 cells dealt with compound **2** at 3.75, 7.50, and 15 μM for 72 h respectively were stained with JC-1, meanwhile untreated cells were used as control. The percentage of green fluorescence increased (0.12%, 25.11%, 36.70%, and 64.80%) in a concentration-dependent manner was observed in Fig. 7. The results demonstrated that **2** could induce apoptosis in HL-60 cells through mitochondrial-related pathway.

## Methods

**General experimental procedures.** Optical rotations were measured on Rudolph Autopol-V digital polarimeter and Jasco P-2000 polarimeter. UV spectra were recorded using a Shimadzu UV-2201 spectrometer. IR spectra were recorded on a Bruker IFS-55 spectrometer (using a KBr disk method). ECD spectra were measured



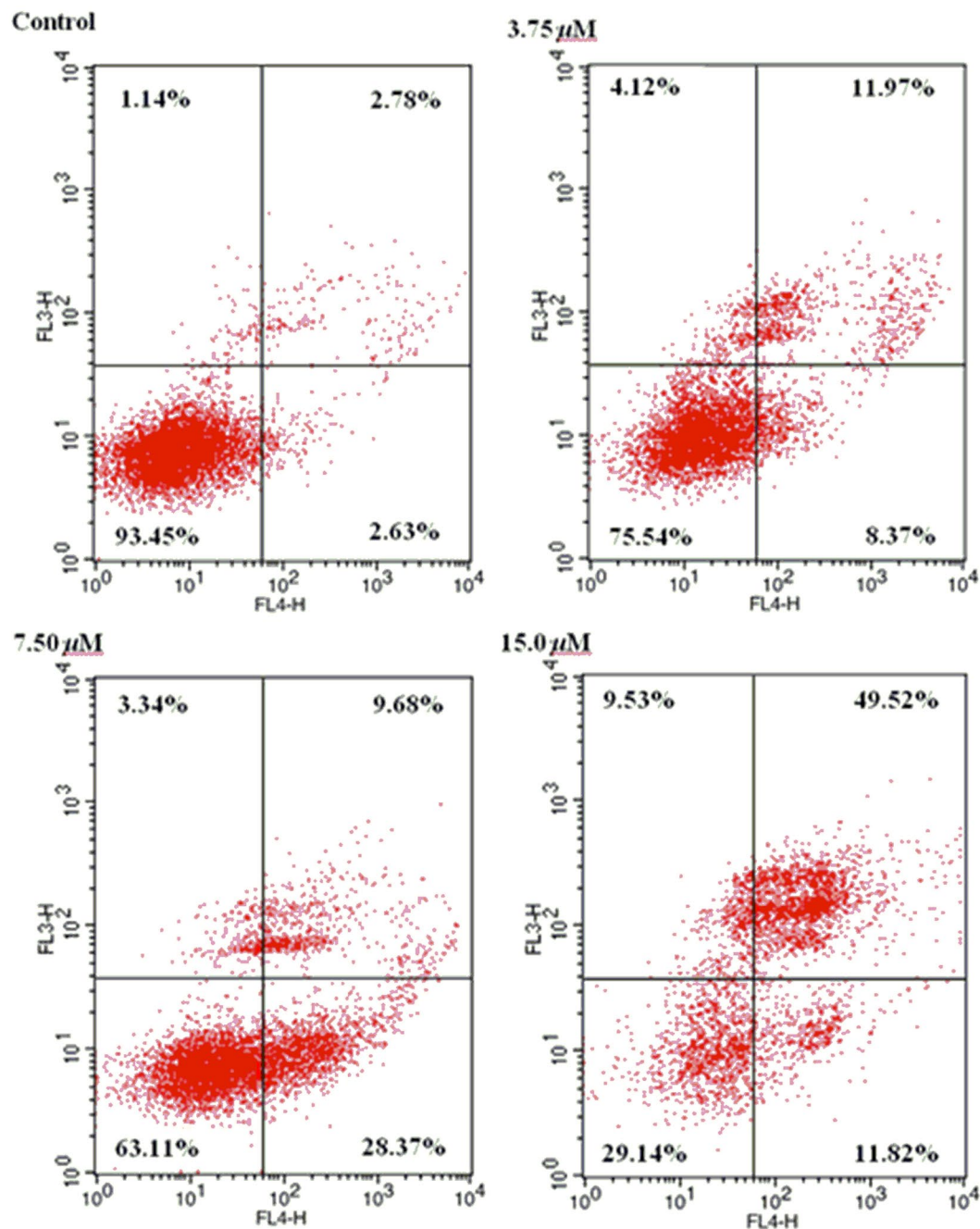


**Figure 6.** Induction of apoptosis by 2 in HL-60 cells.

on Bio-logic MOS 450 spectropolarimeter. 1D and 2D NMR spectra were acquired with Bruker ARX-300 and AV-600 NMR spectrometers using solvent signals ( $\text{CDCl}_3$ :  $\delta_{\text{H}}$  7.26/ $\delta_{\text{C}}$  77.16;  $\text{CD}_3\text{OD}$ :  $\delta_{\text{H}}$  3.31/ $\delta_{\text{C}}$  49.00), with tetramethylsilane (TMS) as an internal standard. HRESIMS data were obtained using Bruker micro-TOFQ-Q mass spectrometer. LC-MS analysis was performed with Thermo Fisher LCQ Fleet Ion Trap LC/MS<sup>n</sup>, and ESI-IT-MS spectra were performed on a Thermo LCQ Advantage MAX Fleet mass spectrometer. A Shimadzu LC-6 AD equipped with a SPD-20A (UV/DAD) detector was used for HPLC. The chiral HPLC isolation was accomplished on Daicel Chiralpak IB column ( $4.6 \times 250$  mm,  $5 \mu\text{m}$ ; Daicel Chemical Ltd, Tokyo, Japan). Column chromatography (CC) were performed with silica (100–200 and 200–300 mesh, Qingdao Haiyang Chemical Co., Ltd., Qingdao, China), neutral alumina (100–200 mesh, Sinopharm Chemical Reagent Co. Ltd., Shanghai, China), ODS ( $50 \mu\text{m}$ , YMC Co. Ltd., Kyoto, Japan), and Sephadex LH-20 (GE Healthcare, Sweden). TLC analyses were carried out with glass plate precoated silica gel ( $\text{GF}_{254}$ ; Qingdao Haiyang Chemical Co., Ltd., Qingdao, China). Spots were visualized under UV light or by spraying with 10%  $\text{H}_2\text{SO}_4$  in 95% EtOH followed by heating or with bismuth potassium iodide solution.

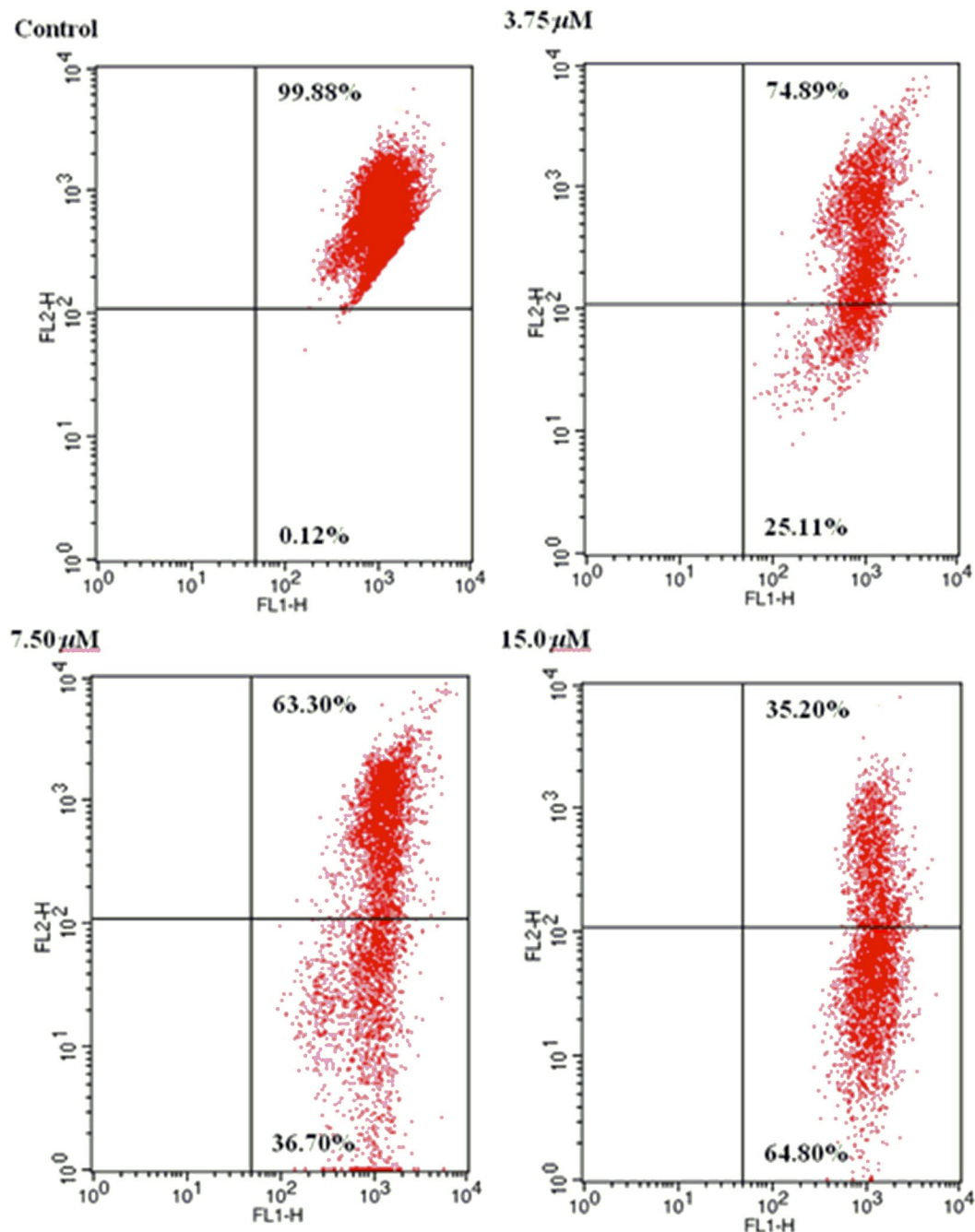


**Figure 7.** Effect of **2** on the mitochondrial membrane potentials in HL-60 cells.

**Plant materials.** The plant material was purchased from Anguo Medicines Ltd (Hebei), China, in November 2013, and was identified as the aerial parts of *Macleaya cordata* (Willd.) R. Br. by Prof. Jincui Lu (School of Traditional Chinese Materia Medica, Shenyang Pharmaceutical University, Shenyang, China). The voucher sample (BLH-20131108) was deposited in the Department of Natural Products Chemistry, Shenyang Pharmaceutical University, Shenyang, China.

**Extraction and isolation.** The air-dried aerial parts of *M. cordata* (40.0 kg) were extracted with 95% ethanol (400 L) under reflux 2 times, and 75% ethanol ( $1 \times 400$  L), each time for 2 h, respectively. After the solvent was removed under reduced pressure, the crude extract (14.6 kg) was suspended in  $H_2O$ , successively partitioned with  $CH_2Cl_2$  and *n*-BuOH, to afford  $CH_2Cl_2$ , *n*-BuOH and aqueous extracts. Part of the  $CH_2Cl_2$  extract (500 g) was subjected to silica gel column chromatography (CC) and eluted with petroleum ether (60–90 °C)–acetone (100:5, 100:10, 100:20, 100:50, 1:1 and 0:100, v/v) to yield six crude fractions (Fr. A–Fr. F). Fr. A was subsequently loaded onto a silica gel column using petroleum ether–EtOAc (100:0, 100:3, 100:5, 100:8, 100:20, v/v) as the eluent to give five subfractions (Fr. A1–Fr. A5). Fr. A2 was applied to neutral alumina CC eluting with petroleum ether–EtOAc,



and further purified by preparative TLC (PTLC) to afford **4** (4.0 mg). Fr. D was further subjected to ODS CC with MeOH–H<sub>2</sub>O (50:50, 60:40, 65:35, 70:30, 80:20, 90:10, v/v) as the mobile phase to give subfractions (Fr. D1–Fr. D6). The residue of Fr. D1 and Fr. D4 after recrystallization was separated by Sephadex LH-20 CC eluting with CH<sub>2</sub>Cl<sub>2</sub>/MeOH (1:1, v/v) to yield total alkaloids (23.9 g) based on TLC analysis. The total alkaloids fraction was further subjected to ODS CC (MeOH–H<sub>2</sub>O, 30:70 to 90:10, v/v). The fraction of 40% methanol elution was recrystallized to give **5** (4.5 mg). The fraction of 75% methanol elution was separated by performing repeated neutral alumina, silica gel, Sephadex LH-20 CC, and PTLC to yield **1** (5.0 mg), and **3** (7.5 mg). Fr. E was subjected to silica gel CC eluted with CH<sub>2</sub>Cl<sub>2</sub>–MeOH (100:0, 200:1, 100:1, 100:2, v/v) to afford four subfractions Fr. E1–Fr. E4. Fr. E1 was subjected to ODS CC eluting with MeOH–H<sub>2</sub>O gradient system, and further recrystallization to yield **6** (30 mg), and then performed on Sephadex LH-20 CC eluting with CH<sub>2</sub>Cl<sub>2</sub>/MeOH (1:1, v/v) to afford **2** (6.0 mg). The *n*-BuOH extract (185 g) was separated on macroporous resin (D101) using EtOH–H<sub>2</sub>O (30:70, 50:50, 70:30, 95:5, v/v) to give four subfractions Fr. G–Fr. J. Fr. H was subjected to ODS CC with MeOH–H<sub>2</sub>O gradient eluting, and the part of 20% MeOH eluting was further purified by reversed-phase preparative HPLC (ODS; 5 μm, 250 × 20 mm; MeOH/H<sub>2</sub>O/DEA, 63:37:0.05, v/v/v; flow rate, 5.0 mL/min) to afford **7** (35 mg, *t*<sub>R</sub> = 45 min).

Chiral separation of **1**, **2**, and **3** was performed on Daicel chiralpak IB column (250 × 4.6 mm), eluted with *n*-hexane–EtOH–DEA (40: 60: 0.1, v/v/v), flow rate 1.0 mL/min to yield **1a** (1.1 mg, *t*<sub>R</sub> 5.930 min), **1b** (1.1 mg, *t*<sub>R</sub> 8.022 min), **2a** (1.5 mg, *t*<sub>R</sub> 5.813 min), **2b** (1.5 mg, *t*<sub>R</sub> 12.305 min), **3a** (1.7 mg, *t*<sub>R</sub> 12.087 min), and **3b** (1.7 mg, *t*<sub>R</sub> 8.074 min), respectively.

Macleayin F (**1**). White amorphous powder. UV (CH<sub>2</sub>Cl<sub>2</sub>) λ<sub>max</sub> (log ε): 227 (4.6), 287 (4.6) nm. IR (KBr) ν<sub>max</sub>: 2790, 1656, 1616, 1486, 1462, 941 cm<sup>-1</sup>. (+)-HRESIMS *m/z* 701.2491 [M + H]<sup>+</sup> (calcd for C<sub>41</sub>H<sub>37</sub>N<sub>2</sub>O<sub>9</sub>, 701.2494).

(+)-Macleayin F (**1a**). [α]<sub>D</sub><sup>20</sup> + 274 (c 0.07, MeOH); ECD (MeOH) λ<sub>max</sub> (Δε) 224 (+9.4), 243 (–22.6), 268 (–3.9), 300 (–7.9) nm.

(–)-Macleayin F (**1b**). [α]<sub>D</sub><sup>20</sup> – 248 (c 0.07, MeOH); ECD (MeOH) λ<sub>max</sub> (Δε) 221 (–13.5), 243 (+24.8), 269 (+3.4), 300 (+7.5) nm.

Macleayin G (**2**). White amorphous powder. UV (CH<sub>2</sub>Cl<sub>2</sub>) λ<sub>max</sub> (log ε): 229 (4.6), 286 (4.6) nm. IR (KBr) ν<sub>max</sub>: 2794, 1652, 1619, 1491, 1458, 938 cm<sup>-1</sup>. (+)-HRESIMS *m/z* 717.2799 [M + H]<sup>+</sup> (calcd for C<sub>42</sub>H<sub>41</sub>N<sub>2</sub>O<sub>9</sub>, 717.2807).

(+)-Macleayin G (**2a**). [α]<sub>D</sub><sup>20</sup> + 238 (c 0.10, MeOH); ECD (MeOH) λ<sub>max</sub> (Δε) 222 (+15.9), 241 (–30.3), 264 (–6.8), 283 (–14.3) nm.

(–)-Macleayin G (**2b**). [α]<sub>D</sub><sup>20</sup> – 210 (c 0.10, MeOH); ECD (MeOH) λ<sub>max</sub> (Δε) 223 (–19.4), 241 (+36.0), 265 (+7.3), 283 (+15.1) nm.

Macleayin H (**3**). White amorphous powder. UV (MeOH) λ<sub>max</sub> (log ε): 232 (4.6), 287 (4.6) nm. IR (KBr) ν<sub>max</sub>: 2798, 1658, 1617, 1485, 1463, 939 cm<sup>-1</sup>. (+)-HRESIMS *m/z* 701.2485 [M + H]<sup>+</sup> (calcd for C<sub>41</sub>H<sub>37</sub>N<sub>2</sub>O<sub>9</sub>, 701.2494).

(+)-Macleayin H (**3a**). [α]<sub>D</sub><sup>20</sup> + 71 (c 0.11, MeOH); ECD (MeOH) λ<sub>max</sub> (Δε) 204 (+19.3), 233 (–24.0), 271 (–0.2), 291 (–5.7) nm.

(–)-macleayin H (**3b**). [α]<sub>D</sub><sup>20</sup> – 94 (c 0.11, MeOH); ECD (MeOH) λ<sub>max</sub> (Δε) 205 (–17.2), 233 (+19.3), 276 (+0.4), 291 (+6.0) nm.

Sanguinarine (**4**). Red amorphous powder. <sup>1</sup>H NMR (400 MHz, CD<sub>3</sub>OD) δ<sub>H</sub>: 9.97 (1 H, s, H-6), 8.67 (1 H, d, *J* = 8.8 Hz, H-10), 8.57 (1 H, d, *J* = 8.9 Hz, H-11), 8.25 (1 H, d, *J* = 8.9 Hz, H-12), 8.18 (1 H, s, H-4), 7.98 (1 H, d, *J* = 8.8 Hz, H-9), 7.60 (1 H, s, H-1), 6.54 (2 H, s, –OCH<sub>2</sub>O-2,3), 6.28 (2 H, s, –OCH<sub>2</sub>O-7,8), 4.97 (3 H, s, N-CH<sub>3</sub>). <sup>13</sup>C NMR (150 MHz, CD<sub>3</sub>OD) δ<sub>C</sub>: 107.0 (C-1), 150.8 (C-2), 150.9 (C-3), 105.0 (C-4), 122.0 (C-4a), 132.9 (C-4b), 52.8 (N-CH<sub>3</sub>), 151.0 (C-6), 111.4 (C-6a), 148.3 (C-7), 149.6 (C-8), 121.3 (C-9), 118.3 (C-10), 129.2 (C-10a), 127.7 (C-10b), 119.7 (C-11), 133.3 (C-12), 134.3 (C-12a), 104.3 (–OCH<sub>2</sub>O-2,3), 106.5 (–OCH<sub>2</sub>O-7,8).

Chelerythrine (**5**). Yellow amorphous powder. <sup>1</sup>H NMR (400 MHz, CD<sub>3</sub>OD) δ<sub>H</sub>: 9.99 (1 H, s, H-6), 8.71 (1 H, d, *J* = 9.0 Hz, H-10), 8.68 (1 H, d, *J* = 9.2 Hz, H-11), 8.24 (1 H, d, *J* = 9.0 Hz, H-9), 8.23 (1 H, d, *J* = 9.2 Hz, H-12), 8.21 (1 H, s, H-4), 7.59 (1 H, s, H-1), 6.28 (2 H, s, –OCH<sub>2</sub>O-2,3), 4.30 (3 H, s, 7-OCH<sub>3</sub>), 4.15 (3 H, s, 8-OCH<sub>3</sub>), 5.01 (3 H, s, N-CH<sub>3</sub>). <sup>13</sup>C NMR (100 MHz, CD<sub>3</sub>OD) δ<sub>C</sub>: 107.1 (C-1), 151.8 (C-2), 150.8 (C-3), 105.1 (C-4), 121.9 (C-4a), 132.6 (C-4b), 52.9 (N-CH<sub>3</sub>), 152.1 (C-6), 119.9 (C-6a), 147.6 (C-7), 151.8 (C-8), 127.5 (C-9), 121.0 (C-10), 130.2 (C-10a), 127.2 (C-10b), 119.5 (C-11), 132.7 (C-12), 134.4 (C-12a), 104.3 (–OCH<sub>2</sub>O-2,3), 62.8 (7-OCH<sub>3</sub>), 57.6 (8-OCH<sub>3</sub>).

Protopine (**6**). Colourless tetragonal crystal (CH<sub>2</sub>Cl<sub>2</sub>: MeOH = 1:1). <sup>1</sup>H NMR (400 MHz, CDCl<sub>3</sub>) δ<sub>H</sub>: 6.90 (1 H, s, H-1), 6.69 (1 H, d, *J* = 7.8 Hz, H-12), 6.66 (1 H, d, *J* = 7.8 Hz, H-11), 6.64 (1 H, s, H-4), 5.95 (2 H, s, –OCH<sub>2</sub>O-2,3), 5.92 (2 H, s, –OCH<sub>2</sub>O-9,10), 3.78 (2 H, br s, H-13), 3.58 (2 H, br s, H-8), 2.2–3.2 (4 H, br s, H-5, 6), 1.91 (3 H, s, N-CH<sub>3</sub>). <sup>13</sup>C NMR (100 MHz, CDCl<sub>3</sub>) δ<sub>C</sub>: 108.3 (C-1), 146.5 (C-2), 148.1 (C-3), 110.6 (C-4), 132.9 (C-4a), 31.9 (C-5), 57.9 (C-6), 50.9 (C-8), 118.0 (C-8a), 146.0 (C-9), 146.1 (C-10), 106.9 (C-11), 125.2 (C-12), 129.1 (C-12a), 46.6 (C-13), 195.1 (C-14), 136.3 (C-14a), 101.3 (–OCH<sub>2</sub>O-2,3), 101.0 (–OCH<sub>2</sub>O-9,10), 41.6 (N-CH<sub>3</sub>).

Allocryptopine (**7**). White amorphous powder. <sup>1</sup>H NMR (400 MHz, CDCl<sub>3</sub>) δ<sub>H</sub>: 6.95 (1 H, s, H-1), 6.91 (1 H, d, *J* = 8.2 Hz, H-12), 6.80 (1 H, d, *J* = 8.2 Hz, H-11), 6.63 (1 H, s, H-4), 5.94 (2 H, s, –OCH<sub>2</sub>O-2,3), 3.86 (3 H, s, 10-OCH<sub>3</sub>), 3.78 (3 H, s, 9-OCH<sub>3</sub>), 3.73 (2 H, br s, H-13), 3.0–3.4 (2 H, br s, H-8), 2.2–3.0 (4 H, br s, H-5, 6), 1.86 (3 H, s, N-CH<sub>3</sub>). <sup>13</sup>C NMR (100 MHz, CDCl<sub>3</sub>) δ<sub>C</sub>: 110.6 (C-1), 146.2 (C-2), 148.2 (C-3), 109.4 (C-4), 136.2 (C-4a), 32.5 (C-5), 57.7 (C-6), 50.3 (C-8), 128.7 (C-8a), 151.7 (C-9), 147.6 (C-10), 110.8 (C-11), 127.9 (C-12), 129.8 (C-12a), 46.5 (C-13), 193.5 (C-14), 133.0 (C-14a), 101.3 (–OCH<sub>2</sub>O-2,3), 60.9 (9-OCH<sub>3</sub>), 55.8 (10-OCH<sub>3</sub>), 41.4 (N-CH<sub>3</sub>).

**Antiproliferative activity.** The HL-60 (human leukaemia cell lines), MCF-7 (human breast cancer cell lines), A-549 (human lung adenocarcinoma cell lines) used in this study were purchased from America Type Culture Collection, ATCC (Rockville, MD, USA). All were cultured in RPMI-1640 medium (Gibco, New York, NY, USA) supplemented with 100 U/mL penicillin, 100 μg/mL streptomycin, 1 mM glutamine and 10% heat-inactivated fetal bovine serum (Gibco) at 37 °C in humidified atmosphere with 5% CO<sub>2</sub>. Cytotoxic activity was evaluated by the trypan blue method against HL-60, and MTT assay against MCF-7 and A-549.

**Cell cycle study.** HL-60 cells in logarithmic growth were plated in 6-well plates and incubated for 24 h, then incubated with different concentrations (0, 3.75, 7.50, 15.0  $\mu\text{M}$ ) of **2** (DMSO only as control) at 37 °C for 72 h. The cells were washed with ice-cold PBS buffer, and then collected, fixed with 70% EtOH at –4 °C for 24 h. The fixed cells were washed with ice-cold PBS and then were treated with 100  $\mu\text{L}$  RNase A at 37 °C for 30 min, and finally stained with 400  $\mu\text{L}$  propidium iodide (PI) in the dark at 4 °C for 30 min. The cycle distribution analysis was performed using a flow cytometer (FACS Calibur, Becton-Dickinson, America).

**Cell apoptosis analysis.** HL-60 cells in logarithmic growth were plated in 6-well plates and incubated for 24 h, then incubated with different concentrations (0, 3.75, 7.50, 15.0  $\mu\text{M}$ ) of **2** (DMSO only as control) at 37 °C for 72 h. The cells were washed twice with ice-cold PBS buffer, and then collected. 500  $\mu\text{L}$  binding buffer suspension cells were added, and finally double stained Annexin V–APC/7-AAD at room temperature for 15 min in the dark. The apoptotic cells were detected to analyze apoptosis by flow cytometry.

**Mitochondrial membrane potential assay.** HL-60 cells in logarithmic growth were plated in 6-well and incubated for 24 h, then incubated with different concentrations (0, 3.75, 7.50, 15.0  $\mu\text{M}$ ) of **2** (DMSO only as control) at 37 °C for 48 h. The cells were washed with ice-cold PBS buffer, subsequently collected and adjusted the cells concentration to  $1 \times 10^6/\text{ml}$ , and finally stained according to the manufacturer's instruction (Keygen, KGA601, Nanjing, China) with JC-1. The percentage of green fluorescence was detected by the flow cytometry to analyze the cells apoptosis and collapsed mitochondrial membrane potentials.

## References

1. Qing, Z. X. *et al.* Structural speculation and identification of alkaloids in *Macleaya cordata* fruits by high-performance liquid chromatography/quadrupole-time-of-flight mass spectrometry combined with a screening procedure. *Rapid Commun. Mass Spectrom* **28**, 1033–1044 (2014).
2. Zeng, J. G. *et al.* Integration of transcriptome, proteome and metabolism data reveals the alkaloids biosynthesis in *Macleaya cordata* and *Macleaya microcarpa*. *PLoS One* **8**, 1–18 (2013).
3. Liu, M. *et al.* *In vitro* assessment of *Macleaya cordata* crude extract bioactivity and anticancer properties in normal and cancerous human lung cells. *Exp. Toxicol. Pathol.* **65**, 775–787 (2013).
4. Yu, X. L. *et al.* Alkaloids from the tribe Bocconieae (Papaveraceae): A chemical and biological review. *Molecules* **19**, 13042–13060 (2014).
5. Sai, C. M. *et al.* Two pairs of enantiomeric alkaloid dimers from *Macleaya cordata*. *Org. Lett.* **17**, 4102–4105 (2015).
6. Qing, Z. X. *et al.* Research progress on mass spectra fragmentation behaviour of alkaloids in *Macleaya cordata*. *Tradit. Herb. Drugs* **44**, 2929–2939 (2013).
7. Wu, Z. D. *et al.* Enantiomeric lignans and neolignans from *Phyllanthus glaucus*: Enantioseparation and their absolute configurations. *Sci. Rep.* **6**, <https://doi.org/10.1038/srep24089> (2016).
8. Luo, Q. *et al.* ( $\pm$ )-Sinensilactam A, a pair of rare hybrid metabolites with Smad3 phosphorylation inhibition from *Ganoderma sinensis*. *Org. Lett* **17**, 1565–1568 (2015).
9. Wang, K. B. *et al.* A series of  $\beta$ -carboline alkaloids from the seeds of *Peganum harmala* show G-quadruplex interactions. *Org. Lett.* **18**, 3398–3401 (2016).
10. Sai, C. M. *et al.* Racemic alkaloids from *Macleaya cordata*: structural elucidation, chiral resolution, and cytotoxic, antibacterial activities. *RSC Adv* **6**, 41173–41180 (2016).
11. Li, D. H. *et al.* Synthesis, biological activity, and apoptotic properties of NO-donor/enmein-type *ent*-kauranoid hybrids. *Int. J. Mol. Sci.* **17**, <https://doi.org/10.3390/ijms17060747> (2016).
12. Tran, T. D. *et al.* Lignans from the Australian endemic plant *Austrobaileya scandens*. *J. Nat. Prod.* **79**, 1514–1523 (2016).
13. Luo, R. *et al.* Synthesis and biological evaluation of baicalein derivatives as potent antitumor agents. *Bioorg. Med. Chem. Lett.* **24**, 1334–1338 (2014).
14. Yu, X. L. *et al.* Usnic acid derivatives with cytotoxic and antifungal activities from the lichen *Usnea longissimi*. *J. Nat. Prod.* **79**, 1373–1380 (2016).
15. Kang, W. J. *et al.* New chalcone and pterocarpoid derivatives from the roots of *Flemingia philippinensis* with antiproliferative activity and apoptosis-inducing property. *Fitoterapia* **112**, 222–228 (2016).
16. Zhao, N. *et al.* Antiproliferative activity and apoptosis inducing effects of nitric oxide donating derivatives of evodiamine. *Bioorg. Med. Chem.* **24**, 2971–2978 (2016).

## Acknowledgements

The work was financially supported by the National Natural Science Foundation of China (Grant No. 81172958), the Shandong Natural Science Foundation (No. ZR2017LC003), and the Foster Foundation of Jining Medical University (No. JYP 201716). We thank Prof. Jincai Lu of School of Traditional Chinese Materia Medica, Shenyang Pharmaceutical University for identification of the plant. We gratefully acknowledge Mr. Yi Sha and Mrs. Wen Li, Department of Analytical Testing Center, Shenyang Pharmaceutical University, for measurements of the NMR data.

## Author Contributions

S.C. and H.H. conceived the project, and designed the experiments. S.C. performed the main experiments, data analyzes, and wrote the manuscript; L.S. assisted the chiral HPLC resolutions; S.C., L.Z. and H.H. analyzed the spectroscopic data; L.D., H.T., and G.Y. performed the antiproliferative activity and mechanism experiments. S.C. and H.H. revised and polished this manuscript. All authors reviewed the manuscript.

## Additional Information

**Supplementary information** accompanies this paper at <https://doi.org/10.1038/s41598-017-15423-4>.

**Competing Interests:** The authors declare that they have no competing interests.

**Publisher's note:** Springer Nature remains neutral with regard to jurisdictional claims in published maps and institutional affiliations.



**Open Access** This article is licensed under a Creative Commons Attribution 4.0 International License, which permits use, sharing, adaptation, distribution and reproduction in any medium or format, as long as you give appropriate credit to the original author(s) and the source, provide a link to the Creative Commons license, and indicate if changes were made. The images or other third party material in this article are included in the article's Creative Commons license, unless indicated otherwise in a credit line to the material. If material is not included in the article's Creative Commons license and your intended use is not permitted by statutory regulation or exceeds the permitted use, you will need to obtain permission directly from the copyright holder. To view a copy of this license, visit <http://creativecommons.org/licenses/by/4.0/>.

© The Author(s) 2017